Hindawi
International Journal of Chemical Engineering
Volume 2022, Article ID 9378712, 12 pages
https://doi.org/10.1155/2022/9378712

Research Article

Comparative Investigation on Two Synthesizing Methods of Zeolites for Removal of Methylene Blue from Aqueous Solution

Misikir Tamiru Asefa and Gebisa Bekele Feyisa

Department of Material Science and Engineering, Adama Science and Technology University, Adama 1818, Ethiopia

Correspondence should be addressed to Gebisa Bekele Feyisa; gebisabek12@gmail.com

Received 5 August 2021; Accepted 12 January 2022; Published 12 February 2022

Academic Editor: Senthil Kumar Ponnusamy

Organic dyes discharged from industries have significant effect on ecosystem and health of human being because of their toxicity and appearing colour in the wastewater. Absorption method is a more preferable method than other wastewater treatment methods due to its characteristics of being eco-friendly, simple, and efficient. Zeolites are among the porous materials often used as absorbent of organic dye from wastewater. However, wide use of zeolite has been limited due to its expensive precursors and synthesized methods (i.e., hydrothermal method which needs expensive autoclave). In this work, cheap and widely available precursors aluminum from waste food packaging aluminum foil and low cost silica from sugar cane bagasse ash were used to synthesized zeolite without hydrothermal method (Z-B), where hydrothermally synthesized zeolite (Z-A) was used as a reference. The XRD patterns revealed that Z-B was sodalite octahydrate zeolite and Z-A was zeolite Linde Type A (LTA). The morphology and type of bond in both zeolites were investigated by SEM and FTIR. The synthesized zeolites were used as absorbents for absorbing methylene blue (MB) from aqueous solutions. The MB removal efficiency of the synthesized zeolites was evaluated by using UV-Visible spectroscopy. The results indicate that the absorption capacities of Z-B and Z-A were 3.5 mg/g and 3.9 mg/g at 40 mg/L, respectively. Optimum removal efficiencies of both zeolites were observed at PH of 7 and adsorbent dosage of 0.005 mg/L. The stabilities of both zeolites were tested three times. The absorption isotherms of sodalite octahydrate zeolite and zeolite LTA were effectively fitted with the Freundlich and Langmuir modes. Moreover, the absorption kinetics of both zeolites follow pseudo-second-order kinetics. Therefore, nonhydrothermally synthesized zeolite is alternative absorbent for dye removal due to its safety, cheap cost, using low cost and widely available precursors, and using easy and safe synthesizing method.

1. Introduction

Water is the most abundant and essential resource for life; life cannot be sustained beyond a few days without water [1, 2]. However, the distribution of water on the Earth's surface is extremely uneven and also it is contaminated by different types of impurities from different sources such as 2,4-Dinitrophenol (DNP) [3], heavy metals [2], and organic dyes [4]. The discharges from the industries are the most responsible contaminants; for instance, dye effluents are discharged from manufacturing, dyeing, printing, and textile industries [5]. Due to the increase in disposal of wastewater, many methods were proposed for wastewater treatment. The most common methods for dyes removal are chemical precipitation [6], flotation [7], flocculation [8], ion exchange [9], chemical oxidation [10], reverse osmosis [11], ultrafiltration [11], electrodialysis [12], and adsorption [13, 14]. Adsorption is a preferable method compared to other methods due to its easy operation, low cost, flexibility in design, high efficiency, availability, high-quality treated effluent, and its recyclability [4]. Some of the recently reported absorbents for removal of organic dyes from wastewater are carbon-based adsorbent materials [15], sugar cane bagasse [16], rice husk [17], magnetic multiwalled carbon nanotubes-loaded alginate [18], silica supported chitosan/glutaraldehyde [19], pomegranate peels based activated carbon [20], and other organic natural materials [21, 22]. Zeolites are among the best adsorbents because they are composed of three-dimensional crystalline and hydrated aluminosilicates made from the interlinked tetrahedra of silica $(SiO_4)^{4+}$ and

Table 1: The lists of raw materials and synthesizing methods of zeolites.

N/s	Raw materials	Synthesizing methods	Applications	References
1	Coal fly ash	Hydrothermal	Desulphurization of wastewater	[26]
2	Rice husk ash	Hydrothermal	CO_2	[27]
3	Textile waste ash	Hydrothermal	Pb	[28]
4	Bagasse fly ash	Hydrothermal	Heavy metals	[29]
5	Kaolin	Hydrothermal	---	[27]

alumina $(A1O_4)^{5+}$ [23]; in addition to this, zeolites have big scientific and industrial significance because of their good ion exchange properties, high surface area, nontoxicity, low cost, abundance, and a hydrophilic characteristic [5, 23]. In fact, there are natural zeolites which are less applicaple compared to the synthetic one because of impurities triggered inside the pores [24]. The common method of synthesizing zeolites is the hydrothermal method [25]. However, the hydrothermal method requires expensive autoclave and it is an unsafe method because it needs high pressure and temperature for a long time. In addition to this, everywhere unavailable precursors such as sources of aluminum oxides and silicon dioxides were used to fabricate zeolite [25]. In order to widely use zeolite for many applications, comprehensively available and low-cost raw materials and cheap and effective synthesizing method are substantial. For instance, recently reported lists of raw materials and synthesizing method for fabricating zeolite are reviewed as shown in Table 1. All the mentioned raw materials were used as sources of sodium silicate, but sodium aluminate salt was used as source sodium aluminate which is somehow expensive. In addition to this, the synthesizing method (i.e., the hydrothermal method) requires expensive autoclave which is not available particularly in developing countries. In this work, comparative study of two synthesizing methods such as coprecipitation and hydrothermal methods for synthesizing zeolites which were used for removal of Methylene blues (MB) from aqueous solution was carried out. In addition to this, the bagasse ash was used as source of sodium silicates and food package aluminum foil wastes were turned to the source of sodium aluminate. To our knowledge, no works had been reported on cost free raw materials and comparative study on synthesizing methods of zeolites. The results indicate that the removal efficiency of Z-B was comparable to that of Z-A at PH of 7, adsorbent dosage of 0.005 mg/L, contact time of 150 min, and MB concentration of 10 ppm.

2. Materials and Methods

2.1. Materials. The reagents used in this work were of analytical grade. Hydrochloric acid (35% HCl), sodium hydroxide (NaOH), and metaylene blue (MB) were purchased from Loba Chemical Company. Sugar cane bagasse ash for this experiment was collected from Wonji sugar factory, Ethiopia. All aqueous solutions were prepared using distilled water. Test tubes were used to hold MB and zeolites solution. Waste food package aluminum foils were collected from deposed area in Adama city. Laboratory clock was used to measure time, and oven was used for drying the samples. Filter paper was also used to filter the precipitate part from the solution. Knife was used to cut the aluminum foil into pieces. Magnetic stirrer was used to uniformly mix the solutions.

2.2. Methods

2.2.1. Collection and Preparation of Sugar Cane Bagasse Ash. Sugar cane bagasse ash for this experiment was collected from Wonji sugar factory, which is 13 Km far from "Adama" town, Ethiopia. Then, the collected bagasse ash was washed repeatedly with distilled water to remove different impurities, especially salt and organic compounds, sun-dried for 2 days in the laboratory, sieved by 200 μm sieves, and stored at room temperature for the next experiment.

2.2.2. Preparation of Sodium Silicate Solution. To obtain pure sodium silicate solution, sugar cane bagasse ash was used as a silica source which is a waste product of sugar factory burned in furnace for 3 hours at 600°C. Calcination can be used to adjust its chemical composition, particularly by reducing its carbon content. Then SCBA was mixed with sodium hydroxide in a ratio of 1 : 1.3, respectively, followed by burning at 600°C for 1 hour. After cooling down the mixture, it was mixed with 200 ml of distilled water and stirred for 10 hours. Then the solution was filtered by using filter paper to obtain sodium silicate solution.

2.2.3. Preparation of Sodium Aluminate. A waste food packaging Al foil was washed and cut into small pieces. 27 g of the powder was dissolved in 250 ml distilled water with 1 M NaOH. Then, the solution was stirred continuously at 60°C with magnetic stirrer until homogeneous solution is obtained [30].

2.2.4. Synthesis of Zeolite. The prepared sodium aluminate solution in the first part by dissolving Al metal and prepared sodium silicate solution was mixed under fast stirring for 10 hours and then left at room temperature to allow the transformation of the mixture from sol into a gel [31, 32]. The gels were transferred to an oven at 100°C for 24 hours and in the section two samples were prepared. For the preparation of the 1st sample, the solution was put in an autoclave and the 2nd sample solution in the beaker and they are abbreviated as Z-A and Z-B, respectively. Then, dry solids were washed repeatedly by distilled water to drop the pH and then dried in the oven. Finally, dried solids were ground into a powder and subsequently calcined at 550°C for 6 hours.

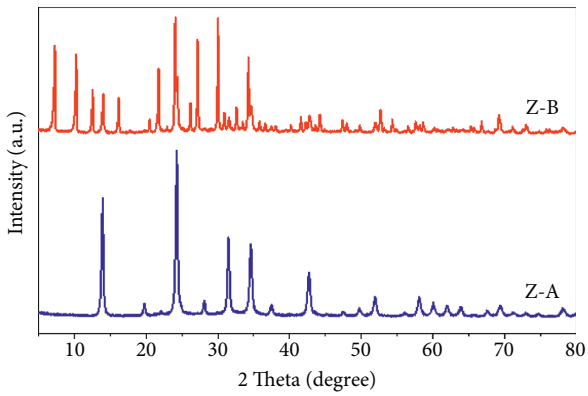

Figure 1: XRD patterns of Z-A and Z-B.

2.3. Characterizations. Determination of the crystal structure of phases purity of each sample was characterized by using X-ray powder diffraction at copper Kα radiation (λCuKa = 1.5418 Å), a scan speed of 3.0000 (deg/min), voltage of 40 kV, current of 30 mA, and scanning range of 10–80°. The surface morphology was analyzed by scanning electron microscopy (SEM) and, finally, the chemical bonds and functional groups of the synthesized zeolite and other samples were determined by using FTIR instrument (FT/IR-6600 type A) with a wavenumber range of 200–4000 cm^{-1}. The absorption efficacies of zeolites were evaluated using UV spectroscopy. Langmuir and Freundlich models were utilized to investigate the nature absorption process. Isothermal models such as pseudo-first-order and pseudo-second-order fitting were also used to observe the nature of both zeolites.

2.4. Adsorption Experiment. The stock solution was prepared in distilled water by using a standard concentration of methylene blue. A series of adsorption tests were carried out at typical equilibrium conditions for the optimization of adsorbents. The mixture was stirred using a magnetic stirrer during all of the experiments and, finally, samples were analyzed by using UV-Visible spectrophotometer (UV-vis-3600 Plus, Shimadzu). Equations (1) and (2) were used to calculate the removal efficiency and adsorption capacity of the adsorbents:

$$q_e = \frac{V(C_o - C_e)}{m}, \quad (1)$$

$$\eta(\%) = \frac{C_o - C_t}{C_o} \times 100, \quad (2)$$

where q_e(mg/g) is the equilibrium adsorption capacity, C_o is the initial concentration of methylene blue, C_e (mg/L) is the concentration of methylene blue at equilibrium time, C_t is the concentration of methylene blue at a given time, V is the volume of solution, m is mass of the adsorbent, and η is removal efficiency.

3. Result and Discussion

3.1. XRD Analysis. Figure 1 shows the XRD results of Z-A and Z-B. In Z-A, the diffraction peaks at angles of $2\theta = 13.99°$, 19.8°, 24.3°, 31.5°, 34.6°, 37.4°, 42.7°, and 58.09° correspond to the (100), (200), (211), (310), (222), (321), (411), and (440) crystallographic planes, indicating sodalite octahydrate zeolite. These results are aligned with the results reported in [33]. In addition to this, the crystal structure of Z-A was compared with the standard zeolite material and it was found that they have similar structures. The XRD pattern of Z-B was also indicated in Figure 1. Diffraction peaks of Z-B were observed at angles of $2\theta = 7.3°$, 10.3°, 12.6°, 16.2°, 21.7°, 24.1°, 27.2°, 30°, and 34.2° corresponding to the (100), (001) (101), (110), (101), (101), (210), (001), and (220) crystallographic planes. These data revealed that Z-B is zeolite LTA that is matched with standard of zeolite LTA. We can conclude that the synthesis of zeolite by using different techniques may give different types of zeolite. But, in both cases of zeolites, no considerable amounts of amorphous phases were observed. Here, even though the type of nonhydrothermally synthesized zeolite has different crystal structure as compared with hydrothermal synthesized zeolite, obtaining zeolite without using expensive autoclave is important in order to reduce the cost and for safety issue.

The crystalline sizes of Z-A and Z-B particles were calculated to be around 23.14 nm and 49.73 nm, respectively, using the Scherrer formula, according to the following equation [34]:

$$D = \frac{K\lambda}{\beta \cos \theta}, \quad (3)$$

where $\lambda = 0.15406$ nm (wavelength of X-ray), $K = 0.9$ (Scherrer constant), D is crystalline size (nm), and = FWHM (full width at half maximum). As is expected, the crystal size of hydrothermally synthesized zeolite was smaller than that of nonhydrothermally synthesized one because of the high pressure in the autoclave. Practically, as particle size decreases, the surface area of the material increases, which promotes the absorption of the pollutants in the wastewater [31]. The effect of crystal size on the removal efficiency will be addressed in Section 3.2.

3.2. SEM Analysis. Figure 2 shows the morphologies of the synthesized zeolites Z-A and Z-B at different magnification. Z-A shows interconnected porous structure with an average particle size less than 24 nm as indicated in Figure 2(a). Similarly, porous structure having interconnection was observed in case Z-B as shown in Figure 2(b). In both cases, spherical-like structures were observed at magnification of 1000x. For the distinct zeolite types, it is reported that different crystal shapes of zeolite are probably associated with different raw materials and preparation methods applied ([32], [33]). Here, although the synthesizing methods were different, the precursors were the same for both zeolites. As a result, a cluster of spherical shapes were observed in both zeolites.

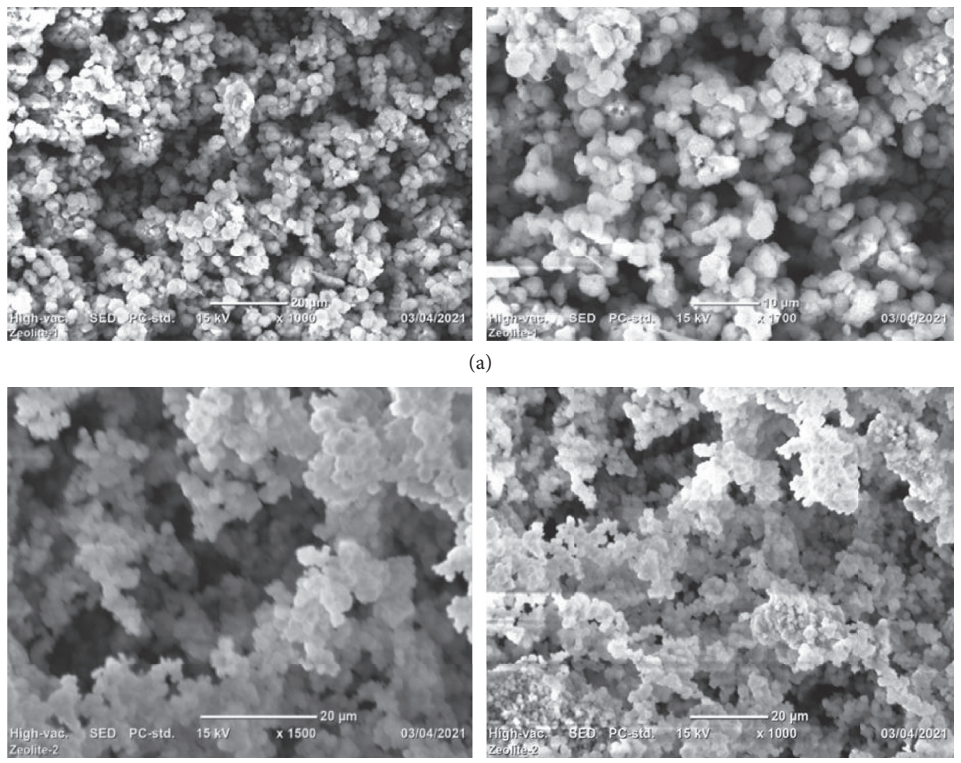

Figure 2: SEM image of (a) Z-A and (b) Z-B at different magnification.

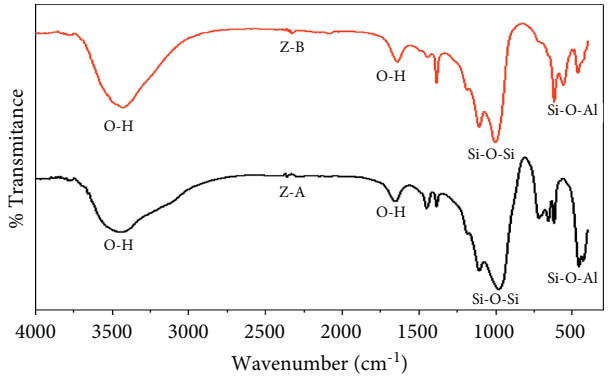

Figure 3: FTIR spectra of Z-A and Z-B.

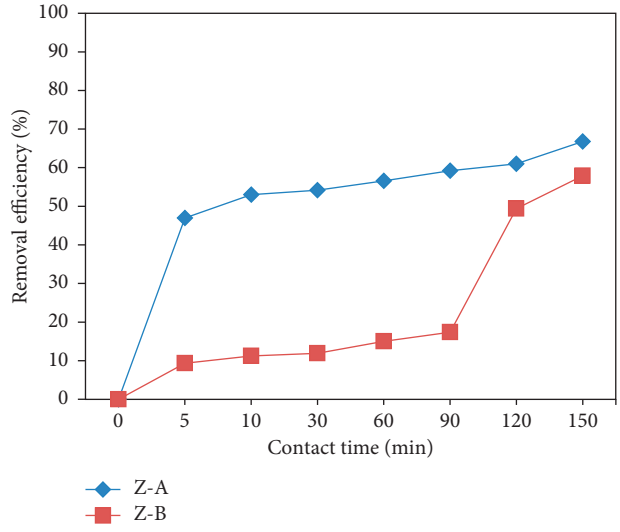

Figure 4: Effect of contact time on removal efficiency of Z-A and Z-B.

3.3. FTIR Analysis. The FTIR spectra of Z-A and and Z-B are shown in Figure 3. The FTIR results showed almost similar spectra of packs with different intensity. In the fingerprint region, the spectrum shows a broad and intense band around 1000 cm^{-1}, showing that the characteristic of antisymmetric stretching vibration of the Si-O-Si and a less intense band around 789 cm^{-1} is due to Si-O-Si symmetric stretching vibrations; this has the same stretching as reported in [35]. Both synthesized zeolites show peaks around 3500 cm^{-1} and 1650 cm^{-1}, which corresponds to the stretching of the hydroxyl groups (OH-) from adsorbed water molecules. The sharpness of the peaks could determine the amount of water (H_2O) molecule adsorbed on the surface of the samples, which in turn can be used to estimate the amount of the hydroxyl functional groups present in the sample as indicated in other research [34]. Other functional groups that exist in the samples are Si-O-Si, indicated by the absorption band at 1020 cm^{-1}, Al-O indicated by peak at 770 cm^{-1}, and Si-O-Al, indicated by the presence of an absorption band at the region between 420 and 494 cm^{-1}. Concerning the existence of functional groups Si, O, and Al observed in the spectrum, it was then concluded that the formation of the

zeolite framework was confirmed by the FTIR results as indicated in [36].

3.4. Adsorption Performance Analysis. The efficiency of adsorbent in water purification is affected by many factors such as contact time, initial concentration of impurity, adsorbent dose, and pH [37, 38]. In this section, the adsorbent performance is studied with respect to those parameters. Similar to the intrinsic properties of the absorbents, the external factors mentioned have a significant impact on the absorbing properties of absorbents.

3.4.1. Effect of Contact Time on Removal Efficiency of Absorbent. Figure 4 shows the effect of the contact time on the MB removal efficiency by both Z-A and Z-B. The adsorption of methylene blue by Z-A and Z-B at room temperature, initial methylene blue concentration of 10 ppm, and adsorbent dosage (Z-A and Z-B) of 3 g/L were used to study the effect of contact time for 150 minutes on the removal efficiency of adsorbents. The adsorptions of methylene blue were slow for both Z-A and Z-B with respect to time because of the low capacity of adsorbents to adsorb; however, adsorption of MB increases as time increases, and this is due to the fact that the occupation of available vacant active sites on the surface of the adsorbents needs enough time to intercalate inside the zeolites. However, as shown in Figure 5, at lower contact time, the removal efficiency of Z-A was higher than that of Z-B because of its small crystal size indicated in the XRD results; however, as time increases, the removal efficiency of both zeolite types shows a comparable result, as shown in Figure 4. At the cost of using expensive autoclave and high temperature that are related to safety issues, the difference in the removal efficiency in the two zeolites was insignificant.

3.4.2. Effect of Initial Concentrations. Figures 5(a) and 5(b) show absorbance of Z-A and Z-B with function wavelength of 200–800 nm and concentration of methylene blue of 10–40 pmm). In both figures, the absorbance at specific wavelength increases as the MB concentration increases, and this is due to large absorption of visible light by MB in the solution. Figure 6 indicates effect of dye concentration on removal efficiency of Z-A and Z-B. For both zeolites, the removal efficiency of methylene blue decreases as the concentration of methylene blue increases from 10 ppm to 40 ppm because, at low initial concentration of methylene blue, there are many adsorption sites, so that there is high removal efficiency, but as the dyes' concentration increases, all the active sites of both zeolites are occupied; thus there is little removal efficiency. Figure 6 shows the impact of the initial concentration of the dyes on the adsorption capacity (q_e (mg/g)). As indicated in this figure, the amount of absorbed dyes (mg) per g increases as the initial concentration of the dyes increases because the active sites of Z-A and Z-B adsorbents were enclosed by much more methylene blue. Thus, adsorbed MB is increased due to the formation of gradient concentration between aqueous solution and adsorbent surface [37, 39, 40]. Here also the MB removal efficiencies of Z-A and Z-B were comparable.

Table 2 shows relative absorption capacities of various absorbents. As indicated in Table 1, the absorption capacities of zeolite Linde Type A and sodalite octahydrate zeolite were comparable.

3.4.3. Effect of Mass of Adsorbent. Figure 6 shows the absorbance of Z-A and Z-B with function of wavelength and mass of absorbent (1–5 g). The absorbances of both zeolites showed the same trends; that is, as mass of absorbent increases, the absorbance decreases because more MB is removed by the zeolites. Figure 7 indicates the removal efficiency of Z-A and Z-B with function mass absorbents. The removal efficiency of both zeolites increases with the increases of its mass because of more adsorption sites introduced to the solution. By increasing the number of adsorbent particles, there is more methylene blue attached, also reported in [46, 47]. The removal efficiencies of both zeolites were also comparable.

3.4.4. Effect of pH Value. Figure 7 shows the effect of pH of the solution on the removal efficiency Z-A and Z-B. The results revealed that the removal efficiencies of both zeolites were significantly dependent on the pH values because at low pH value the adsorbent shows less removal efficiency due to the fact that highly acidic hydrogen ion competes with MB ions to occupy the sites of the adsorbent [48], and at higher pH value, which is a high alkali region, there is a generation of more hydroxyl sites, which also decreases the adsorption efficiency of the material [49]. So the optimum pH value was obtained to be 7. Here also the removal efficiencies of both zeolites have minor differences.

3.4.5. Recyclability Study. Figures 8(a) and 8(b) show recyclability of Z-A and Z-B for three time tests. In both figures, the blue bar indicates that after absorbent recovered from solution by filtering, it was washed by distilled water, and red bar indicates the recovered absorbent washed by strong acid. The results showed the amount of MB adsorbed onto Z-A and Z-B for the three cycles, by using different regeneration techniques [50, 51]. The first method was done by washing the adsorbents using distilled water several times; then they were centrifuged and finally oven-dried. In the cause of using this method, it was difficult to regenerate the samples because of the MB ion triggered inside the pores of adsorbent. The other method of reusability done on this work was using of strong acid (0.005 mol of HCl) to wash the adsorbent, after which it was centrifuged and dried. The result indicated that the prepared adsorbent can be easily regenerated by using acid rather than water, so acid treated samples have better reusability and stability than those which were washed by water. In both cases, Z-A and Z-B show the same trends of recyclability.

3.5. Adsorption Isotherm Analysis. The equilibrium model used to characterize equilibrium behavior by describing the amount of adsorbate adsorbed as a function of gas or liquid

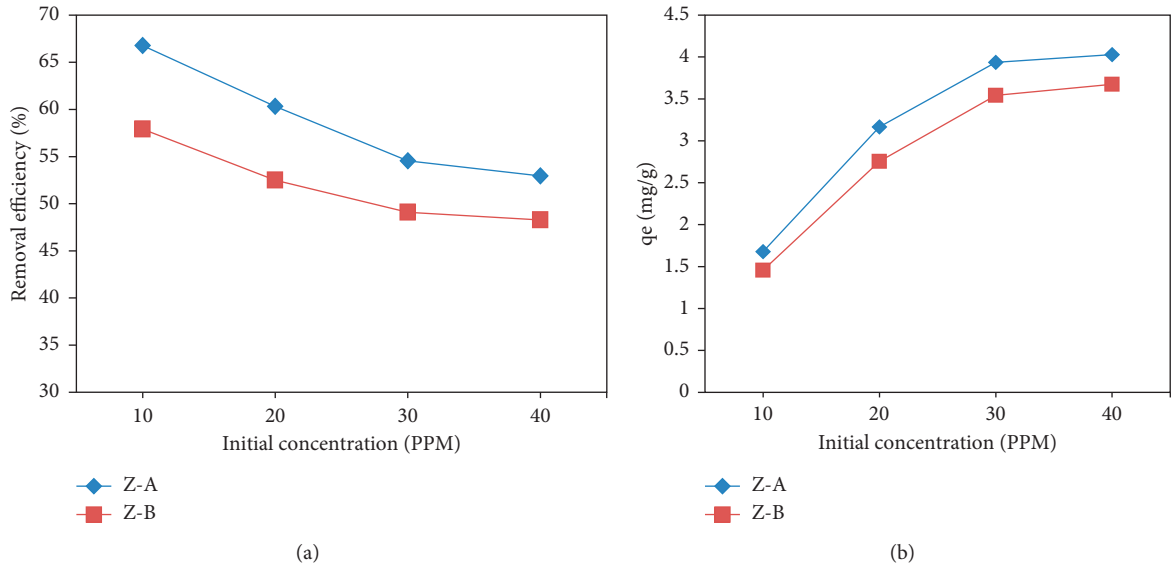

Figure 5: (a) Effect of dye concentration on removal efficiency and (b) adsorption capacity of Z-A and Z-B.

at a constant temperature is called an isotherm [52]. The basis of the study of the adsorption process is the adsorption isotherm model. The adsorption isotherm is the main source for measuring the adsorption of substances. Several equilibrium models have been used to explain the adsorption process, such as Langmuir, Freundlich, Temkin, Slips, Hill, Radke-Prausnitz, and Flory-Huggins isotherms. Langmuir and Freundlich adsorption isotherms are the most commonly used models [52]. The Langmuir model assumes that the surface of the adsorbent for removing adsorbate is uniform and flat, and the adsorbed molecules or ions have no interaction. On the other hand, the Freundlich model assumes that adsorption occurs on an uneven surface, each local adsorption site has its own binding energy, and the strongest binding site is established before the end of the adsorption process [53, 54]. Among them, q_e (mg/g) is the equilibrium adsorption capacity, q_{max} (mg/g) is the maximum adsorption capacity that the adsorbent can achieve, l/mg is the Langmuir adsorption constant, Ce (mg/l) is the equilibrium concentration, K_F is Freund's constant ((mg/g) (l/g)1/n), which represents the binding energy of the adsorbent, and n is the adsorption intensity.

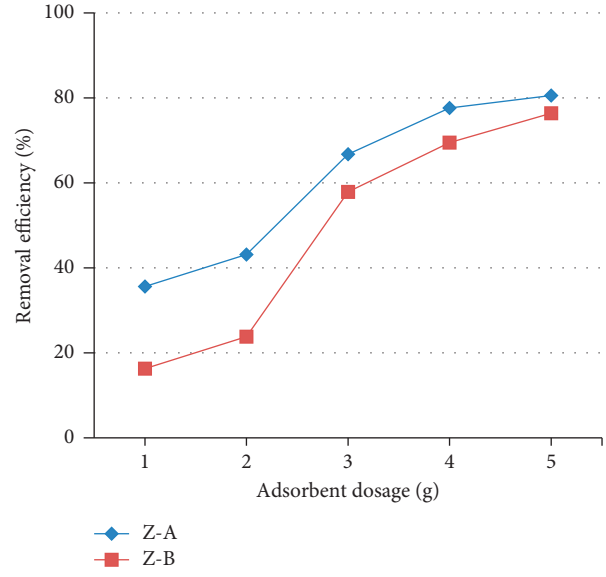

Figure 6: Effect of adsorbent dosage on removal efficiency of Z-A and Z-B.

3.5.1. Langmuir Isotherm Model. Langmuir isotherm on solid surface assumes that adsorption is homogeneous or monolayer adsorption [55]. The Langmuir isotherm model can be described according to the equation in Table 3 to determine adsorption isotherm.

3.5.2. Freundlich Isotherm Model. Freundlich isotherm is an empirical relation between the concentrations of a solute on the surface of an adsorbent to the concentration of the solute present in the liquid [35]. The Freundlich isotherm equation is described in Table 1. Therefore, based on the results shown in Figures 9 and 10, the adsorption data conformed to both the Langmuir and Freundlich isotherms. Both isotherms were apparently best fitted models with a correlation coefficient (R^2) greater than 98; thus, this proves the adsorption of methylene blue on surfaces of Z-A and Z-B due to porous nature of the adsorbent [35]. The maximum adsorption capacity of Z-A towards methylene blue was 4.0299 mg/g and it was 3.678 mg/g for Z-B samples as determined using Langmuir equation. Furthermore, the dimensionless Freundlich constant $n > 1$, which implies adsorption was favorable on heterogeneous surface. Generally, the value of $1/n < 0.5$ implies easy adsorption, and $1/n > 2$ implies difficult adsorption [36]. In this work, the adsorption intensity $(1/n) = 0.609$ and 0.70914 for Z-A and Z-B samples, respectively, and this implied that the adsorption of methylene blue on the surface of zeolite was favorable as the isotherm

Table 2: Relative absorption capacities of various absorbents.

Dye	Absorbent	Absorption capacity (mg/g)	Reference
MB	Bagasse ash	4.41	[41]
MB	Natural zeolite	1.5	[42]
MB	Zeolite Linde Type A	3.9	This work
MB	Sodalite octahydrate zeolite	3.5	This work
MB	ZSM-5 zeolite	4.31	[43]
MB	Rice husk	6	[44]
MB	Activated carbon	4.59	[45]

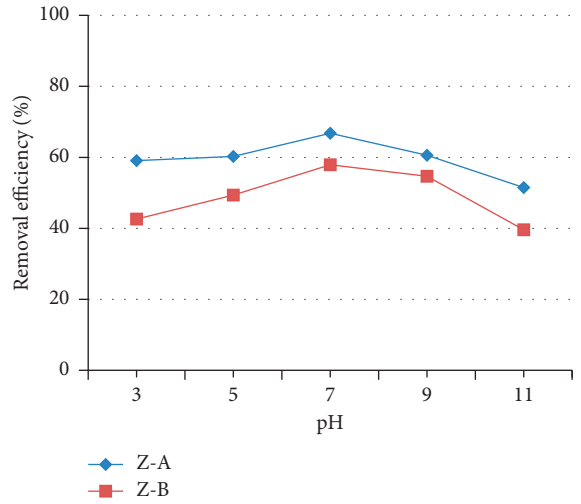

Figure 7: Effect of pH on removal efficiency of Z-A and Z-B.

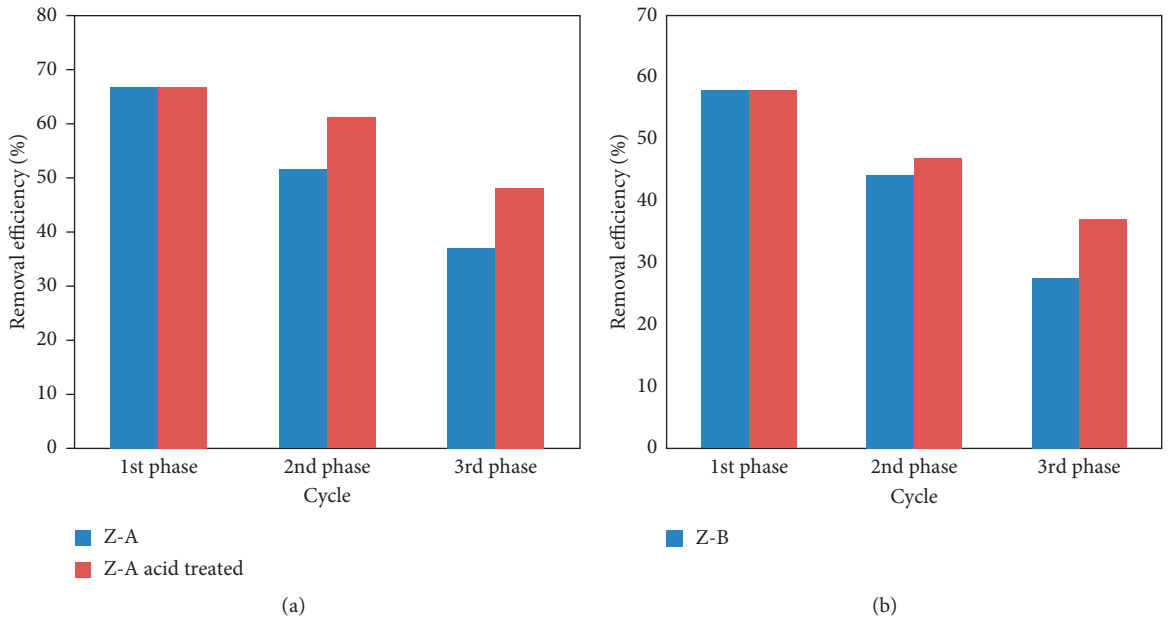

Figure 8: (a) The recyclability of Z-A and (b) the recyclability of Z-B.

Table 3: Langmuir and Freundlich parameters extracted from isotherm models.

Isotherm model	Nonlinear equation	Linear equation	Plot	Reference
Langmuir	$q_e = q_{\max} bc/(1 + bC_e)$	$C_e/q_e = 1/bq_{\max} + C_e/q_e$	C_e/q_e vs C_e	Swensnet et al., [56]
Freundlich	$q_e = K_F C_e^{1/n}$	$\ln q_e = 1/n \ln C_e + \ln k_F$	$\ln q_e$ vs $\ln C_e$	[36]

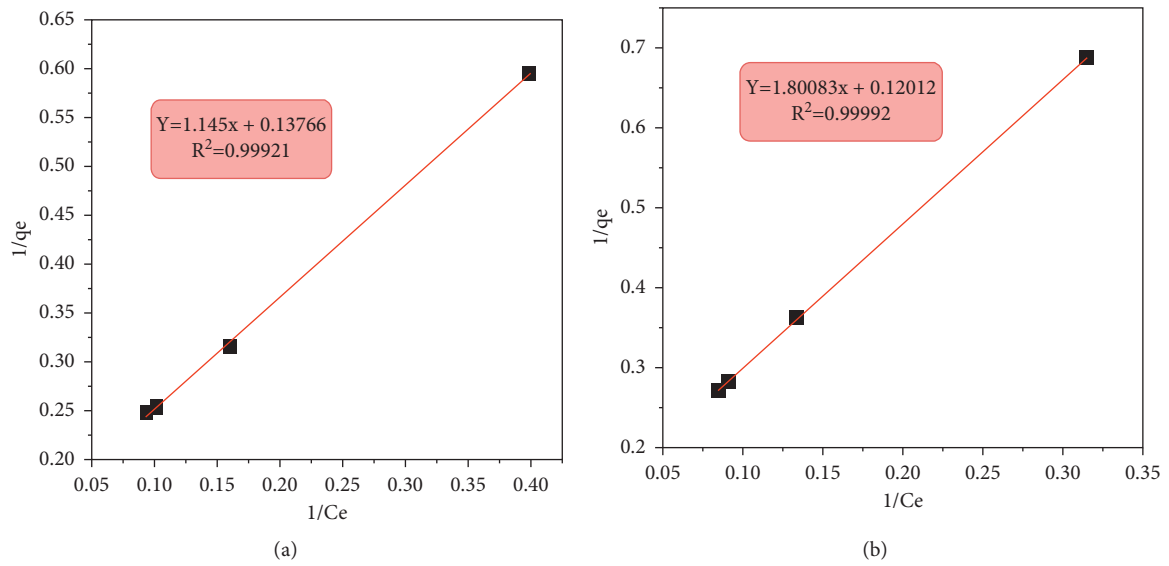

Figure 9: (a) Langmuir isotherm: a plot of $1/q_e$ against $1/C_e$ of sample Z-A. (b) Langmuir isotherm: a plot of $1/q_e$ against $1/C_e$ of sample Z-B.

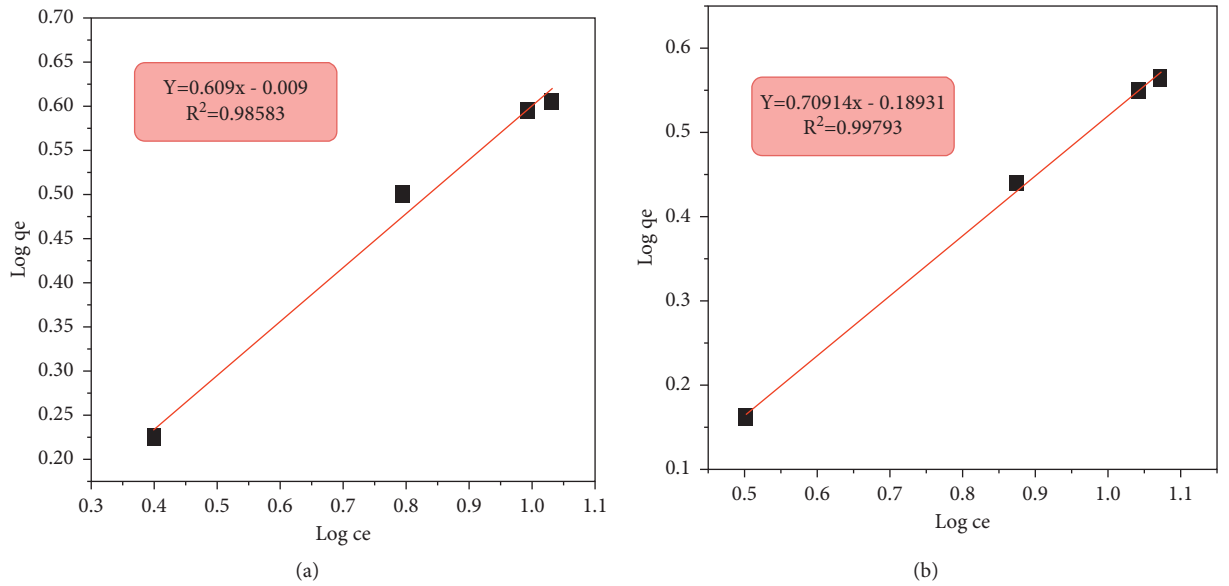

Figure 10: (a) Plot of $\ln(q_e)$ against $\ln(C_e)$ which shows Freundlich isotherm of Z-A. (b) Plot of $\ln(q_e)$ against $\ln(C_e)$ of Freundlich isotherm Z-B.

[57]. So, we can conclude that adsorption was favorable according to both isotherm models.

3.6. Adsorption Kinetics. The study of adsorption kinetics is very important for wastewater purification because it provides important information about process characteristics, reaction forms, and adsorption reaction mechanisms. The adsorption process is mainly described by pseudo-first-order and pseudo-second-order kinetic models based on chemical reaction kinetics [58].

3.6.1. Pseudo-First-Order. Lagergren's pseudo-first-order model is based on the assumption that the rate of change of solute absorption over time is proportional to the difference

Table 4: Equations for pseudo-first-order and pseudo-second-order kinetic models.

Isotherm model	Equation	Plot	Reference
Pseudo-first-order	Log $(qe - qt) = \log qe - K_1/2.303\,t$	Log $(qe - qt)$ vs time	[59]
Pseudo-second-order	$t/qt = 1/K_2 qe^2 + t/qe$	t/qt vs time	[60]

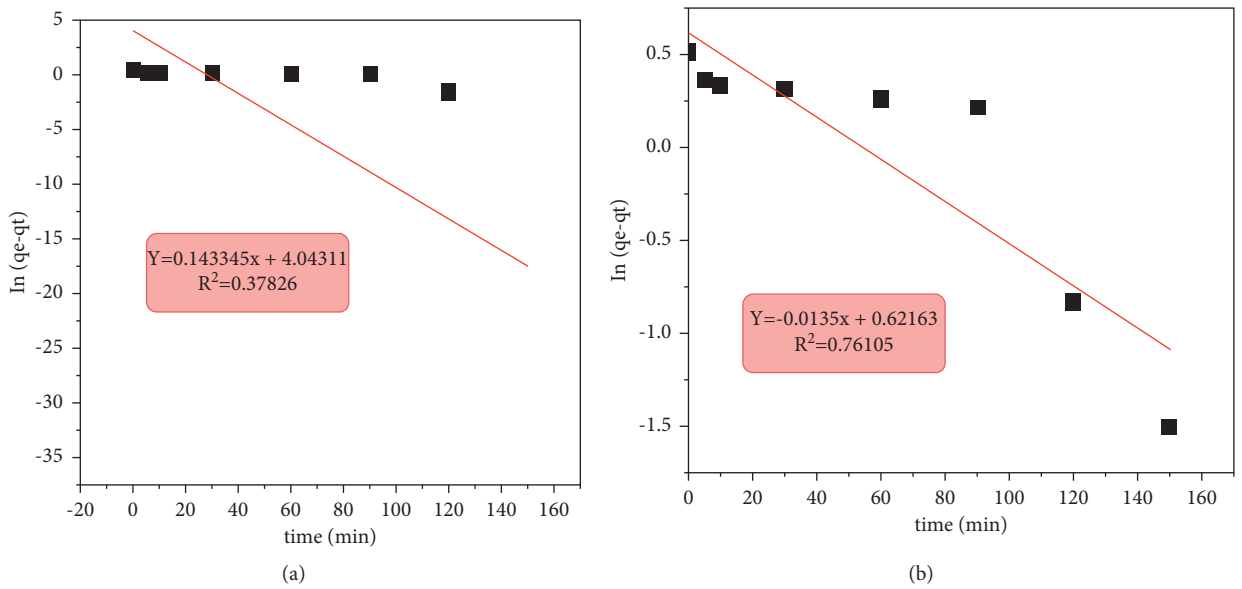

Figure 11: Pseudo-first-order model for (a) Z-A and (b) Z-B samples.

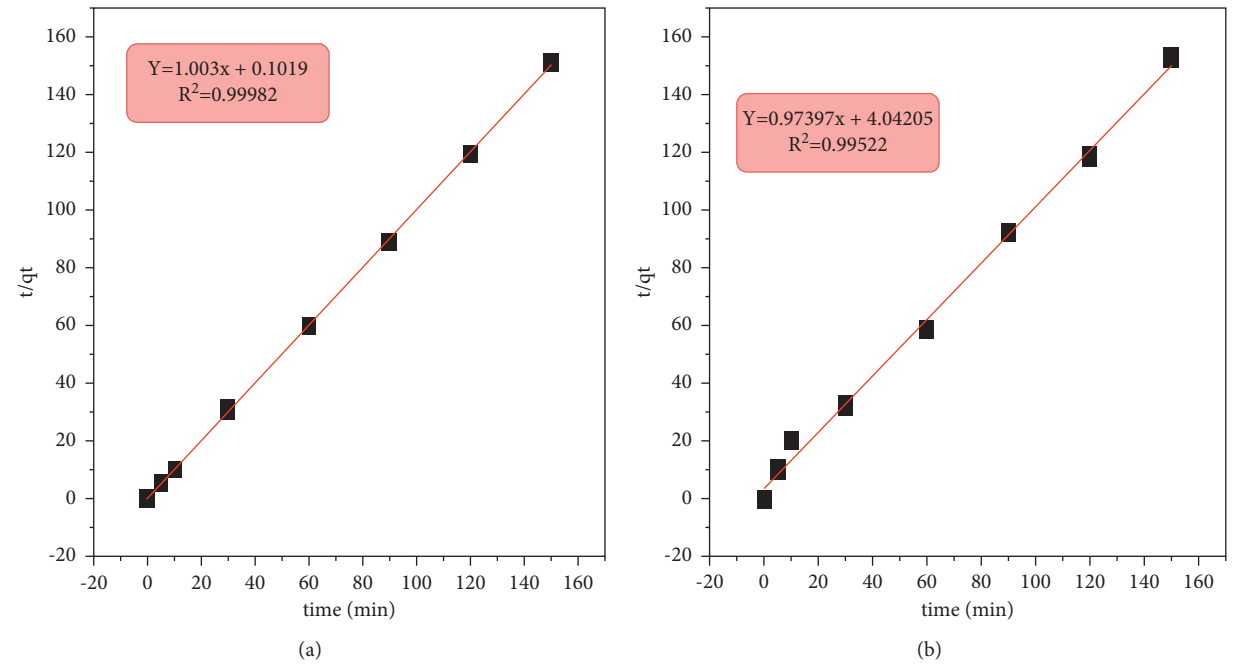

Figure 12: Pseudo-second-order model for (a) Z-A and (b) Z-B samples.

in saturation concentration and the amount of solid absorbed over time, which is usually applied in the early stages of kinetics. When adsorption occurs through interface diffusion, this pseudo-first-order large particle rate equation is usually observed [57, 58]. The pseudo-first-order Lagergren model can be described by the equation shown in Table 4.

According to the pseudo-first-order dynamics, if the adsorption process follows the true first-order kinetics, the

intersection of log (q_e -q_t) and t is equal to the logarithm of q_e, which is determined by experiment or corrected to match the experimental value. In this case, the pseudo-first-order Lagergren equation does not fit the entire adsorption time range as shown in Figure 11.

3.6.2. Pseudo-Second-Order. The pseudo-second-order kinetic model is based on the assumption that the rate-limiting step is chemical adsorption or chemisorption and predicts the behavior over the entire adsorption range. In this state, the adsorption rate depends on the adsorption capacity, not the concentration. An important advantage of this model over first-order storage quantities is that the equilibrium adsorption capacity can be calculated from the model; therefore, there is theoretically no need to evaluate the equilibrium adsorption capacity from the experiment [57, 59–62]. In pseudo-second-order kinetics, the adsorption process follows true second-order kinetics as shown in Figure 12; then the intercept of t/q_e versus t plots had been adjusted to fit the experimental value, so pseudo-second-order kinetics were fitted well for the whole range of adsorption time. In pseudo-first-order kinetic models, there is a big difference in q_e, exp and q_e, cal, which indicates that the adsorption of methylene blue by Z-A and Z-B adsorbent does not obey pseudo-first-order kinetics; on the other hand, the values of q_e, exp, and q_e, cal obtained in pseudo-second-order model are very close. In addition to this, the correlation coefficient (R^2) = 0.76105 and 0.37826, respectively, for Z-A and Z-B in pseudo-first-order kinetics, wile the pseudo-second-order kinetics model showed a higher correlation coefficient (R^2) of 0.99982 and 0.99522 for Z-A and Z-B, respectively, so we can confirm that the pseudo-second-order model is the best fitted model for the adsorbent.

4. Conclusions

Sodalite octahydrate zeolite is an alternative absorbent for removing methylene blue from aqueous solution with respect to zeolite LTA because sodalite octahydrate zeolite was synthesized by solution method, which is a cheap, easy, and safe method, and zeolite LTA was synthesized by the hydrothermal method that requires expensive autoclave. The absorption capacities of sodalite octahydrate zeolite and zeolite LTA were 3.5 mg/g and 3.9 mg/g at 40 mg/L, respectively. The pH values of the solution affect the absorption capacity of both zeolites. The optimum removal efficiencies of both zeolites were observed at pH value of 7. The removal efficiencies of mentioned zeolites increase with increasing of absorbent dosage because absorption active site increases with the scale-up of the absorbent dosage. The stabilities of both absorbents were checked three times and it was found that they were stable. The absorption isotherms of sodalite octahydrate zeolite and zeolite LTA were effectively fitted with the Freundlich and Langmuir models. Moreover, the absorption kinetics of both zeolites follow the pseudo-second-order kinetics [62]

Data Availability

No data were generated during this study.

Conflicts of Interest

The authors declare that they have no conflicts of interest.

References

[1] G. Howard, *Domestic Water Quantity, Service Level and Health*, World Health Organization, Geneva, Switzerland, 2020.

[2] D. Ghernaout, "Increasing trends towards drinking water reclamation from treated wastewater," *World Journal of Applied Chemistry*, vol. 3, no. 1, pp. 1–9, 2018.

[3] A. Azari, M. Yeganeh, M. Gholami, and M. Salari, "The superior adsorption capacity of 2,4-Dinitrophenol under ultrasound-assisted magnetic adsorption system: modeling and process optimization by central composite design," *Journal of Hazardous Materials*, vol. 418, p. 126348, 2021.

[4] S. Wang, H. Li, and L. Xu, "Application of zeolite MCM-22 for basic dye removal from wastewater," *Journal of Colloid and Interface Science*, vol. 295, no. 1, pp. 71–78, 2006.

[5] S. Wang and Z. Zhu, "Characterisation and environmental application of an Australian natural zeolite for basic dye removal from aqueous solution," *Journal of Hazardous Materials*, vol. 136, no. 3, pp. 946–952, 2006.

[6] L. K. Wang, D. A. Vaccari, Y. Li, and N. K. Shammas, "Chemical precipitation," in *Physicochemical Treatment Processes*Springer, Berlin, Germany, 2005.

[7] W. Wójtowicz, "Adsorption of methylene blue and Congo red from aqueous solution by activated carbon and carbon nanotubes," *Water Science and Technology*, vol. 68, no. 10, pp. 2240–2248, 2013.

[8] M. Milichovský and B. Češek, "Surface flocculation as a new tool for controlling adsorption processes," *Adsorption Science and Technology*, vol. 20, no. 9, pp. 883–896, 2002.

[9] F. C. Nachod, *Ion Exchange: Theory and Application*, Elsevier, Amsterdam, Netherlands, 2012.

[10] I. Rashed: Overview on Chemical Oxidation Technology in Wastewater Treatment 1. 2005.

[11] Z. Amjad, "Reverse osmosis: membrane technology, water chemistry, and industrial applications," *Ultrafiltration Handbook*, Technomic Publishing Co. Inc., New York, NY, USA, 1993.

[12] T. Mohammadi, A. Moheb, M. Sadrzadeh, and A. Razmi, "Modeling of metal ion removal from wastewater by electrodialysis," *Separation and Purification Technology*, vol. 41, no. 1, pp. 73–82, 2005.

[13] F. Fu and Q. Wang, "Removal of heavy metal ions from wastewaters: a review," *Journal of Environmental Management*, vol. 92, no. 3, pp. 407–418, 2011.

[14] D. O. Cooney, *Adsorption Design for Wastewater Treatment*, CRC Press, Boca Raton, FL, USA, 1998.

[15] A. Azari, R. Nabizadeh, A. H. Mahvi, and S. Nasseri, "Magnetic multi-walled carbon nanotubes-loaded alginate for treatment of industrial dye manufacturing effluent: adsorption modelling and process optimisation by central composite face-central design," *International Journal of Environmental Analytical Chemistry*, pp. 1–21, 2021.

[16] R.-F. Wang, L.-G. Deng, K. Li, X.-J. Fan, W. Li, and H.-Q. Lu, "Fabrication and characterization of sugarcane bagasse-calcium carbonate composite for the efficient removal of crystal

violet dye from wastewater," *Ceramics International*, vol. 46, no. 17, pp. 27484–27492, 2020.

[17] C. M. Paranhos, "Evaluation of rice husk ash in adsorption of Remazol Red dye from aqueous media," *SN Applied Sciences*, vol. 1, p. 397, 2019.

[18] A. Azari, R. Nabizadeh, A. H. Mahvi, and S. Nasseri, "Integrated Fuzzy AHP-TOPSIS for selecting the best color removal process using carbon-based adsorbent materials: multicriteria decision making vs. systematic review approaches and modeling of textile wastewater treatment in real conditions," *International Journal of Environmental Analytical Chemistry*, pp. 1–16, 2020.

[19] M. H. Fazlzadeh, M. H. Niari, A. Azari, and E. C. Lima, "A novel silica supported chitosan/glutaraldehyde as an efficient sorbent in solid phase extraction coupling with HPLC for the determination of Penicillin G from water and wastewater samples," *Arabian Journal of Chemistry*, vol. 13, no. 9, pp. 7147–7159, 2020.

[20] Y. Rashtbari, S. Hazrati, A. Azari, S. Afshin, M. Fazlzadeh, and M. Vosoughi, "A novel, eco-friendly and green synthesis of PPAC-ZnO and PPAC-nZVI nanocomposite using pomegranate peel: cephalexin adsorption experiments, mechanisms, isotherms and kinetics," *Advanced Powder Technology*, vol. 31, no. 4, pp. 1612–1623, 2020.

[21] M. Tamiru and B. Guta, "Various absorbents and parameters affecting removal of water hardness from wastewater: review," *International Journal of Water and Wastewater Treatment*, vol. 6, no. 3, 2020.

[22] A. E. Burakov, E. V. Galunin, I. V. Burakova et al., "Adsorption of heavy metals on conventional and nanostructured materials for wastewater treatment purposes: a review," *Ecotoxicology and Environmental Safety*, vol. 148, pp. 702–712, 2018.

[23] J. V. Smith, "Definition of a zeolite," *Zeolites*, vol. 4, no. 4, pp. 309-310, 1984.

[24] J. D. Sherman, "Synthetic zeolites and other microporous oxide molecular sieves," *Proceedings of the National Academy of Sciences*, vol. 96, no. 7, pp. 3471–3478, 1999.

[25] J. G. Garcia Mendoza, *Synthesis and Applications of Low Silica Zeolites from Bolivian Clay and Diatomaceous Earth*, Lulea University of Technology, Luleå, Sweden, 2017.

[26] P. Nowak, B. Muir, A. Solińska, M. Franus, and T. Bajda, "Synthesis and characterization of zeolites produced from low-quality coal fly ash and wet flue gas desulphurization wastewater," *Materials*, vol. 14, no. 6, p. 1558, 2021.

[27] Y. Wang, H. Jia, P. Chen, X. Fang, and T. Du, "Synthesis of La and Ce modified X zeolite from rice husk ash for carbon dioxide capture," *Journal of Materials Research and Technology*, vol. 9, no. 3, pp. 4368–4378, 2020.

[28] T. Hussain, A. I. Hussain, S. A. S. Chatha et al., "Synthesis and characterization of Na-zeolites from textile waste ash and its application for removal of lead (Pb) from wastewater," *International Journal of Environmental Research and Public Health*, vol. 18, no. 7, p. 3373, 2021.

[29] J. A. Oliveira, F. A. Cunha, and L. A. M. Ruotolo, "Synthesis of zeolite from sugarcane bagasse fly ash and its application as a low-cost adsorbent to remove heavy metals," *Journal of Cleaner Production*, vol. 229, pp. 956–963, 2019.

[30] N. S. Ahmedzeki, "Waste resources utilization for zeolite a synthesis," *Journal of Chemical Technology & Metallurgy*, vol. 53, no. 2, 2018.

[31] H. Zhang, R. L. Penn, R. J. Hamers, and J. F. Banfield, "Enhanced adsorption of molecules on surfaces of nanocrystalline particles," *The Journal of Physical Chemistry B*, vol. 103, no. 22, pp. 4656–4662, 1999.

[32] H. Strathmann, L. Giorno, and E. Drioli, "Introduction to membrane science and technology," vol. 544, Wiley-VCH, Weinheim, Germany, 2011.

[33] V. C. H. Feng Wiley and C. Weinheim.Feng, "Recent progress in zeolite/zeotype membranes," *Journal of Membrane Science and Research*, vol. 1, no. 2, pp. 49–72, 2015.

[34] S. A. Zygmunt, L. A. Curtiss, L. E. Iton, and M. K. Erhardt, "Computational studies of water adsorption in the zeolite H-ZSM-5," *Journal of Physical Chemistry*, vol. 100, no. 16, pp. 6663–6671, 1996.

[35] H.-K. Chung, W.-H. Kim, J. Park, J. Cho, T.-Y. Jeong, and P.-K. Park, "Application of Langmuir and Freundlich isotherms to predict adsorbate removal efficiency or required amount of adsorbent," *Journal of Industrial and Engineering Chemistry*, vol. 28, pp. 241–246, 2015.

[36] O. Fo and E. Odebunmi, "Freundlich and Langmuir isotherms parameters for adsorption of methylene blue by activated carbon derived from agrowastes," *Advances in Natural and Applied sciences*, vol. 4, pp. 281–288, 2010.

[37] E. S. Mirjavadi, R. Tehrani, and A. Khadir, "Effective adsorption of zinc on magnetic nanocomposite of Fe3O4/zeolite/cellulose nanofibers: kinetic, equilibrium, and thermodynamic study," *Environmental Science and Pollution Research*, vol. 26, no. 32, pp. 33478–33493, 2019.

[38] A. A. Alswata and M. B. Ahmad, "Preparation of zeolite/zinc oxide nanocomposites for toxic metals removal from water," *Results in Physics*, vol. 7, pp. 723–731, 2017.

[39] A. A. Alswata, M. B. Ahmad, N. M. Al-Hada, H. M. Kamari, M. Z. B. Hussein, and N. A. Ibrahim, "Preparation of zeolite/zinc oxide nanocomposites for toxic metals removal from water," *Results in Physics*, vol. 7, pp. 723–731, 2017.

[40] A. Mollahosseini, A. Khadir, and J. Saeidian, "Core-shell polypyrrole/Fe3O4 nanocomposite as sorbent for magnetic dispersive solid-phase extraction of Al+3 ions from solutions: investigation of the operational parameters," *Journal of Water Process Engineering*, vol. 29, p. 100795, 2019.

[41] T. C. Andrade Siqueira, I. Zanette da Silva, A. J. Rubio et al., "Sugarcane bagasse as an efficient biosorbent for methylene blue removal: kinetics, isotherms and thermodynamics," *International Journal of Environmental Research and Public Health*, vol. 17, no. 2, p. 526, 2020.

[42] G. Amin, D. Đorđević, S. Konstantinović, and I. Jordanov, "The removal OF the textile basic dye from the water solution BY using natural zeolite," *Advanced technologies*, vol. 6, no. 2, pp. 67–71, 2017.

[43] S. Radoor, J. Karayil, A. Jayakumar, J. Parameswaranpillai, and S. Siengchin, "Removal of methylene blue dye from aqueous solution using PDADMAC modified ZSM-5 Zeolite as a novel Adsorbent," *Journal of Research Square*, 2021.

[44] L. Ahmad Nasir, Z. U. Zango, U. Armaya'u, and Z. N. Garba, "Rice HUSK as biosorbent for the adsorption OF methylene blue," *Science World Journal*, vol. 14, no. 2, 2019.

[45] H. Seifi and S. Masoum, "Ultrasonically assisted removal of toxic dye using Iranian bituminous coal based-activated carbon: synthesis, characterization, modeling, equilibrium and kinetic studies," *Journal of the Iranian Chemical Society*, vol. 17, no. 11, pp. 2969–2980, 2020.

[46] Z. Rawajfih and N. Nsour, "Thermodynamic analysis of sorption isotherms of chromium(VI) anionic species on reed biomass," *The Journal of Chemical Thermodynamics*, vol. 40, no. 5, pp. 846–851, 2008.

[47] Y. M. Hao, C. Man, and Z. B. Hu, "Effective removal of Cu (II) ions from aqueous solution by amino-functionalized

magnetic nanoparticles," *Journal of Hazardous Materials*, vol. 184, no. 1-3, pp. 392–399, 2010.

[48] K. S. Hui, C. Y. Chao, and S. C. Kot, "Removal of mixed heavy metal ions in wastewater by zeolite 4A and residual products from recycled coal fly ash," *Journal of Hazardous Materials*, vol. 127, no. 1-3, pp. 89–101, 2005.

[49] F. Ji, C. Li, B. Tang, J. Xu, G. Lu, and P. Liu, "Preparation of cellulose acetate/zeolite composite fiber and its adsorption behavior for heavy metal ions in aqueous solution," *Chemical Engineering Journal*, vol. 209, pp. 325–333, 2012.

[50] M. T. Mihajlović, "Kinetics, thermodynamics, and structural investigations on the removal of Pb 2+, Cd 2+, and Zn 2+ from multicomponent solutions onto natural and Fe (III)-modified zeolites," *Clean Technologies and Environmental Policy*, vol. 17, no. 2, pp. 407–419, 2015.

[51] A. A. Alswata, M. B. Ahmad, and T. A. Saleh, "Preparation and characterization of zeolite\zinc oxide-copper oxide nanocomposite: antibacterial activities," *Colloid and Interface Science Communications*, vol. 16, pp. 19–24, 2017.

[52] M. J. Ahmed and S. K. Dhedan, "Equilibrium isotherms and kinetics modeling of methylene blue adsorption on agricultural wastes-based activated carbons," *Fluid Phase Equilibria*, vol. 317, pp. 9–14, 2012.

[53] X. Chen, "Modeling of experimental adsorption isotherm data," *Information*, vol. 6, no. 1, pp. 14–22, 2015.

[54] M. A. Al-Ghouti and D. A. Da'ana, "Guidelines for the use and interpretation of adsorption isotherm models: a review," *Journal of Hazardous Materials*, vol. 393, p. 122383, 2020.

[55] N. Oladoja, C. Aboluwoye, and Y. Oladimeji, "Kinetics and isotherm studies on methylene blue adsorption onto ground palm kernel coat," *Turkish Journal of Engineering and Environmental Sciences*, vol. 32, no. 5, pp. 303–312, 2009.

[56] D. A. Fungaro and M. Bruno, "Adsorption and kinetic studies of methylene blue on zeolite synthesized from fly ash," *Desalination and Water Treatment*, vol. 2, no. 1-3, pp. 231–239, 2009.

[57] B. Bonelli, *Nanomaterials for the Detection and Removal of Wastewater Pollutants*, Elsevier, Amsterdam, Netherlands, 2020.

[58] S. Azizian, "Kinetic models of sorption: a theoretical analysis," *Journal of Colloid and Interface Science*, vol. 276, no. 1, pp. 47–52, 2004.

[59] Y. C. Wong, Y. S. Szeto, W. H. Cheung, and G. McKay, "Pseudo-first-order kinetic studies of the sorption of acid dyes onto chitosan," *Journal of Applied Polymer Science*, vol. 92, no. 3, pp. 1633–1645, 2004.

[60] Y. S. Ho and G. McKay, "Pseudo-second order model for sorption processes," *Process Biochemistry*, vol. 34, no. 5, pp. 451–465, 1999.

[61] H. Swenson and N. P. Stadie, "Langmuir's theory of adsorption: a centennial review," *Langmuir*, vol. 35, no. 16, pp. 5409–5426, 2019.

[62] V. O. Shikuku, C. O. Kowenje, and F. O. Kengara: Errors in Parameters Estimation Using Linearized Adsorption Isotherms: Sulfadimethoxine Adsorption onto Kaolinite Clay. 2018.